Full-duplex transmission of multi-Gb/s subcarrier multiplexing and 5G NR signals in 39 GHz band over fiber and space

Dong-Nhat Nguyen,[1,] Luis Vallejo,[2] Vincenc Almenar,[2] Beatriz Ortega,[2] Pham Tien Dat,[3] Son Thai Le,[4] Jan Bohata, [1] and Stanislav Zvanovec[1*]

[1]*Department of Electromagnetic Field, Czech Technical University in Prague, Technicka 2, 166 27, Czech Republic*
[2]*Instituto de Telecomunicaciones y Aplicaciones Multimedia, ITEAM, Universita Politecnica de Valencia, Valencia 46022, Spain*
[3]*Network Research Institute, National Institute of Information and Communication, Tokyo 184-8795, Japan*
[4]*Nokia Bell Labs, Holmdel, New Jersey 07733, USA*
**Corresponding author: xzvanove@fel.cvut.cz*

Received XX November 2021; revised XX Month, XXXX; accepted XX Month XXXX; posted XX Month XXXX (Doc. ID XXXXX); published XX Month XXXX

We propose a stable full-duplex transmission of millimeter-wave signals over a hybrid single-mode fiber (SMF) and free-space optics (FSO) link for the fifth-generation (5G) radio access networks to accelerate the Industry 4.0 transformation. For the downlink (DL), we transmit 39 GHz subcarrier multiplexing (SCM) signals using variable quadrature amplitude modulation (QAM) allocations for multi-user services. As a proof-of-operation, we experimentally demonstrate the transmission of 3 Gb/s SCM signals (1 Gb/s per user) over a hybrid system consisting of a 10 km SMF and 1.2 m FSO link. For the uplink (UL), satisfactory performance for the transmission of 2.4 Gb/s 5G NR signal at 37 GHz over the hybrid system is experimentally confirmed for the first time. The measured error vector magnitudes for both DL and UL signals using 4/16/64-QAM formats are well below the 3GPP requirements. We also further evaluate by simulation the full-duplex transmission over the system in terms of received optical and RF powers and bit error rate performance. A wireless radio distance of approximately 200 m, which is sufficient for 5G small-cell networks, is estimated for both DL and UL direction under the heavy rain condition, based on the available data from Spain. Furthermore, simulation for the DL direction is conducted to verify the superior performance of the system using variable QAM allocation over uniform QAM allocation. Using a variable modulation allocation, up to five users (2 Gb/s per user) can be transmitted over a hybrid 10 km SMF and 150 m FSO link.

1. INTRODUCTION

Radio access technologies operating at the low radio frequency (RF) regions (i.e., sub-6 GHz) fail to meet the increasing connectivity and latency needs of high-performance industrial use cases, e.g. automated guided vehicle for automatic inspection of production lines, real-time control and inspection systems and remote augmented reality assistance for equipment troubleshooting, maintenance and repair [1].

The fifth-generation (5G) radio access networks (RAN) operating in the millimeter-wave (mmW) bands, i.e. such as 26 GHz (24.25 – 27.5 GHz), 28 GHz (26.5 – 29.5 GHz) and 39 GHz (37 – 40 GHz) bands [2], will make a substantial change. While the 5G spectrum still needs to be harmonized, the 39 GHz band is one of the most widely discussed spectra of 5G mmW communications [3]. However, implementing 39 GHz mmW-based 5G RAN would encounter two key challenges: i) Stringent requirements of high-speed electronic components and signal processing at the transmitter (Tx) side, which makes the mmW signal generation module complex and costly. ii) High propagation loss in free space and large attenuation under rain condition, which requires an increase in the radio transmit power.

To address the first challenge, microwave photonic link (MPL) i.e., radio-over-fiber system, has been considered as an effective solution by both academia community and industrial sectors [4]–[8]. This is because in the MPL-based 5G RAN, all the signal processing, data modulation and optical mmW signal generation are carried out at a central office (CO), which significantly reduces the hardware complexity of the antenna (ANT) site. The optical mmW signal is transmitted over a standard single-mode fiber (SMF) to the small-cell base stations (BSs). Full-duplex MPLs (i.e., DL and UL) are also recently gaining considerable attention [9], [10]. Regarding the optical mmW signal generation, the most effective and simple solution is to use the optical frequency multiplication (OFM) technique based on the Mach-Zehnder

modulators (MZMs) [11]. This method allows for tunable optical mmW signal generation and, therefore, considerably relaxes the high-speed electronic and processing requirements. The first challenge thus can be properly solved.

To circumvent the second challenge, adopting the free-space optical (FSO) communication technology into MPL, defined as hybrid MPL (HMPL), is highly favorable for practical applications. The inclusion of the FSO link can help reduce the RF wireless transmission range, which leads to the benefit of power efficiency and offers stable downlink (DL) and uplink (UL) connections since FSO can operate in bidirectional, unlicensed and electromagnetic interference-immune conditions [12].

A. Related works

Several studies on the mmW HMPL-based 5G RAN have been proposed and experimentally demonstrated. A full-duplex HMPL system using an optical heterodyne method for 60 GHz 16- and 64-QAM signal transmission over a hybrid 25 km SMF, 1 m FSO and 1 m RF wireless link was presented in [13]; however, the data rate (R_b) was limited to 80 Mb/s and 120 Mb/s, respectively. A transmission of 80 Gb/s and 41 Gb/s filter bank multi-carrier signals over the DL and UL direction was carried out in [14] using a 20 km SMF, 1.5 m FSO, and 1 m RF wireless link [14]. However, the DL and UL signals were transmitted separately and complex optical in-phase-quadrature modulators were used for data modulation, which makes the HMPL bulky and costly. The transmission of 26 GHz 5G NR signal over a hybrid system was demonstrated in [15] using 12.5 km SMF, 1 m FSO and 8 m RF wireless link. Nevertheless, only DL transmission was implemented and R_b was limited to 1.2 Gb/s. Also, a HMPL link using an analog MPL approach and photonical doubling scheme with carrier suppression was demonstrated in [16] with the transmission over 10 km SMF and 4 m FSO at 39 GHz using the 5G NR signal. A similar scheme was used in [17] for the mmW signal transmission over up to 50 km SMF, 40 m FSO and 40 m seamless antenna channel at 25 GHz. However, both published works considered only the DL direction. Notably, there are no reported HMPL systems employed (i) low-cost directly modulated laser (DML) for data modulation, (ii) OFM technique to avoid the use of high-frequency RF components, and (iii) composite subcarrier multiplexed (SCM) signals for multiple-user services. In our previous work [18], we employed a DML and OFM technique for the demonstration of three-user transmission over 10 km SMF using the uniform 16-QAM allocation. However, only DL transmission was demonstrated and R_b was limited to 0.8 Gb/s.

B. Contributions

In this paper, we propose a stable multi-Gb/s full-duplex HMPL at 39 GHz band for next-generation 5G mmW RAN for the first time. Examples of the use cases of such an HMPL are presented in Fig. 1, where several applications of the optical fiber and wireless fronthaul network can be seen in a converged radio-optical network for the ubiquitous wireless service. The seamless fiber-FSO system can work as a mobile fronthaul system (extension of an SMF) for consequent transmission of radio signal where the use fiber cable is not possible or too expensive. Note. the FSO link is expected to work as the radio access network (NR). High capacity SCM fronthaul connection can as well provide connection in places such as airports or factories to densify the wireless communication infrastructure. The system can be employed for various applications such as back-up, disaster recovery, last-mile or extension of broadband wireless connectivity. The main contributions of the paper are summarized as follows:

i. We investigated the SCM signal transmission e.g., multi-intermediate frequency (IF) using variable QAM allocations (i.e., each IF band signal is modulated using a different QAM level) to enable high-performance DL multi-user service. The key advantage of using different QAM in each band is that they can better exploit the non-flat frequency response and non-uniform signal to noise ratio of the system. Fast reconfiguration to more robust QAM is essential to minimize the power fading caused by hybrid channel effects (e.g., SMF chromatic dispersion (CD) and FSO atmospheric turbulence (AT)). Depending on the transmission circumstances, each modulation can be adaptively configured to maintain the desirable link operation.

ii. We demonstrated proof-of-concept transmissions of 4 Gb/s single-band (16-QAM) and 3 Gb/s three-band (4/16/64-QAM – 1 Gb/s each) signals at 39 GHz in the DL direction and 2.4 Gb/s 5G NR signal at 37 GHz in the UL direction. The DL and UL signals are simultaneously transmitted over the mutual hybrid SMF-FSO link for the first time.

iii. We estimated the bit error rate (BER) and achievable wireless link range under rain conditions in Spain for both DL and UL direction on the basis of the measured error vector magnitude (EVM) and receiver sensitivity (S_{Rx}) obtained from experiments. We confirmed that under the heavy rain condition in Spain, the system could transmit the SCM and 5G NR signals over a wireless link range of approximately 200 m, which is sufficient for small-cell network coverage.

iv. We provided extensive simulation analysis of variable and uniform QAM SCM signal transmission over the hybrid system with a long FSO link. As a result, we confirmed that by using variable QAM allocation, up to

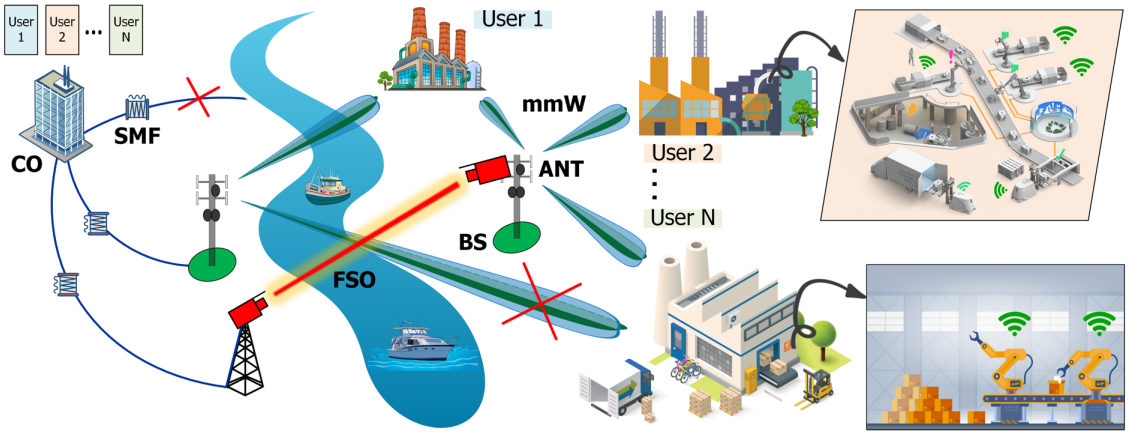

Fig. 1. The proposed 5G mmW RAN infrastructure-based HMPL for delivering multi-Gb/s wireless connectivity to assist manufactoring plants and factories in Industry 4.0 era. CO: central office, SMF: single-mode fiber, FSO: free-space optics, BS: base station, mmW: millimeter-wave and ANT: antenna.

five users (2 Gb/s per user) can be accommodated for the transmission over a hybrid 10 km SMF and 150 m FSO link under a practical AT condition in an outdoor environment. While this is not possible using a uniform modulation allocation scheme.

The remainder of the paper is structured as follows: Section 2 discusses the advantage of FSO channel for future mmW RAN. Section 3 describes the proof-of-concept experimental setup of the proposed full-duplex HMPL. Section 4 provides the experimental results and estimation of RF wireless length for both DL and UL. Section 5 then presents the numerical simulation analysis of DL, highlighting the effectiveness of the variable over the uniform QAM allocations scheme in practical outdoor environments. Finally, section 6 concludes the paper.

2. FSO FOR NEXT-GENERATION MMW RADIO ACCESS NETWORKS

The inclusion of FSO channel into the system brings the advantage of power efficiency in comparison to the RF wireless link. This is because the former uses extremely narrow laser beams while the latter is highly dependent on frequency. At present, compact full-duplex and auto-tracking FSO transceivers with an aperture diameter of 10 cm, narrow beam divergence (θ) of 0.55 mrad and 0.2 mrad operating at λ of 1550 nm and R_b of 1 Gb/s, 10 Gb/s and 30 Gb/s over the corresponding FSO transmission length (L_{FSO}) of 4.4 km, 1.5 km and 1.3 km, respectively, have become commercially available [12].

The link equation for an FSO system regarding the received ($P_{\mathrm{r\_FSO}}$) and transmitted ($P_{\mathrm{t\_FSO}}$) optical beam power can be expressed by [19]:

$$P_{\mathrm{r\_FSO}} = P_{\mathrm{t\_FSO}} \frac{d_{\mathrm{R}}^2}{(d_{\mathrm{T}}+\theta L_{\mathrm{FSO}})^2} 10^{-\alpha_{\mathrm{atm\_FSO}}\frac{L_{\mathrm{FSO}}}{10}} \quad (1)$$

where d_{R} and d_{T} are aperture diameters, which are identical in a full-duplex system, and $\alpha_{\mathrm{atm\_FSO}}$ is the atmospheric attenuation factor, which is about 0.2 dB/km in a clear weather condition (i.e., no rain).

Figure 2(a) shows the relationship of $P_{\mathrm{r\_FSO}}$ and L_{FSO} at a fixed $P_{\mathrm{t\_FSO}}$ of 5 dBm for different practical values of θ. As can be clearly seen, the narrower θ, the lower loss. Comparing at L_{FSO} of 500 m, the corresponding $P_{\mathrm{r\_FSO}}$ for θ of 2 mrad, 0.55 mrad and 0.2 mrad are -16 dBm, -6.5 dBm and -1 dBm, which result in the transmission loss of 21 dB, 11.5 dB and 6 dB, respectively.

On the contrary, RF wireless link suffers a total loss of the propagation path loss (α_{PT}), rain loss (α_{rain}) and atmospheric loss ($\alpha_{\mathrm{atm\_RF}}$), which is strongly dependent upon the RF carrier frequency. Assuming no rain, Fig. 2(b) then presents the total loss as a function of RF wireless length L_{RF} for 39 GHz, 60 GHz and 90 GHz wireless links. Note that, at 39 GHz, 60 GHz and 90 GHz, $\alpha_{\mathrm{atm\_RF}}$ values are about 0.18 dB/km, 15 dB/km and 0.4 dB/km, respectively [20]. We can see that, at L_{RF} of 500 m, the corresponding total losses are 118 dB, 130 dB and 124 dB, which are substantially higher than that of the FSO link. This confirms the feasibility of FSO link in 5G RAN. Note that, the RF wireless link loss can be reduced by adopting a phased array ANT-based autonomous beamforming technology as reported recently for 40 [21] and 60 GHz [22] MPLs.

Since laser beams are highly vulnerable to AT, which is instigated by the random small-scale temperature variations along the FSO link [19], the demodulated signal at the Rx thus experiences the reduction in signal quality (i.e., high EVM) and distortions in QAM constellation diagrams.

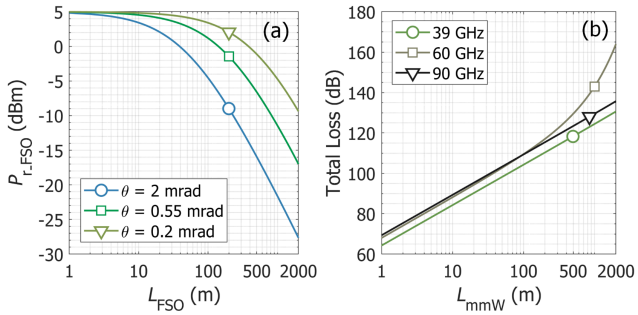

Fig. 2. (a) Dependence of received optical beam power on FSO link length for different values of beam divergence and (b) RF wireless link total loss versus wireless link length at 39 GHz, 60 GHz and 90 GHz in a fair weather condition (i.e., no rain).

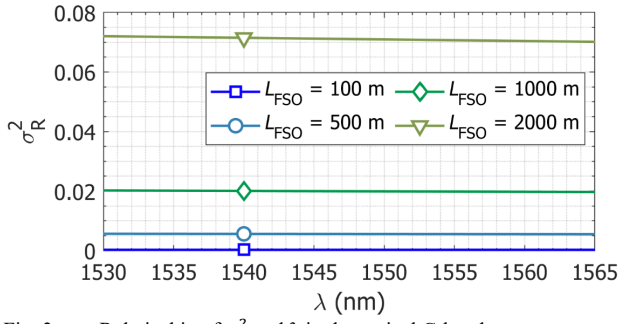

Fig. 3. Relatioship of σ_{R}^2 and λ in the optical C-band spectrum.

The most widely used parameters to determine and categorize the AT strength are the refractive index structure parameter (C_n^2 ($\mathrm{m}^{-2/3}$)), and Rytov variance (σ_{R}^2), in which they are linearly proportional to each other as given by [19]:

$$\sigma_{\mathrm{R}}^2 = 1.23 C_n^2 \left(\frac{2\pi}{\lambda}\right)^{7/6} {L_{\mathrm{FSO}}}^{11/6} \quad (2)$$

In a practical outdoor environment, C_n^2 generally varies from 10^{-17} $\mathrm{m}^{-2/3}$ to 10^{-13} $\mathrm{m}^{-2/3}$ for weak-to-strong AT regimes. According to Eq. (2), we could see that σ_{R}^2 is dependent on λ. Since the proposed full-duplex HMPL works in the optical C-band spectrum, one concern is that the AT effect on DL and UL signal performance might be different. Assuming the practical C_n^2 of 10^{-15} $\mathrm{m}^{-2/3}$, we then present in Fig. 3 the relationship of σ_{R}^2 and λ for different L_{FSO} of 100 m, 500 m, 1000 m and 2000 m. As can be seen, at each L_{FSO}, σ_{R}^2 is almost similar within the optical C-band window. Therefore, the wavelength dependence of AT effect is negligible. Please note in this analysis we do not include fog influence [23] or the role of atmospheric aerosols on the FSO [24].

3. EXPERIMENTAL SETUP

Figure 4(a) illustrates the experimental setup. For the DL direction, in the CO, both single and multiple user signals were evaluated. The latter was generated at different IFs and added together to form a composite SCM signal by using an arbitrary waveform generator (AWG, Tektronix AWG7122C). The multiplexed signal was then electrically amplified by an RF power amplifier (PA-1, Wenteq ABL0300-01-2516) up to 9 dBm. Note that the transmitting power of the all used amplifiers was set to not

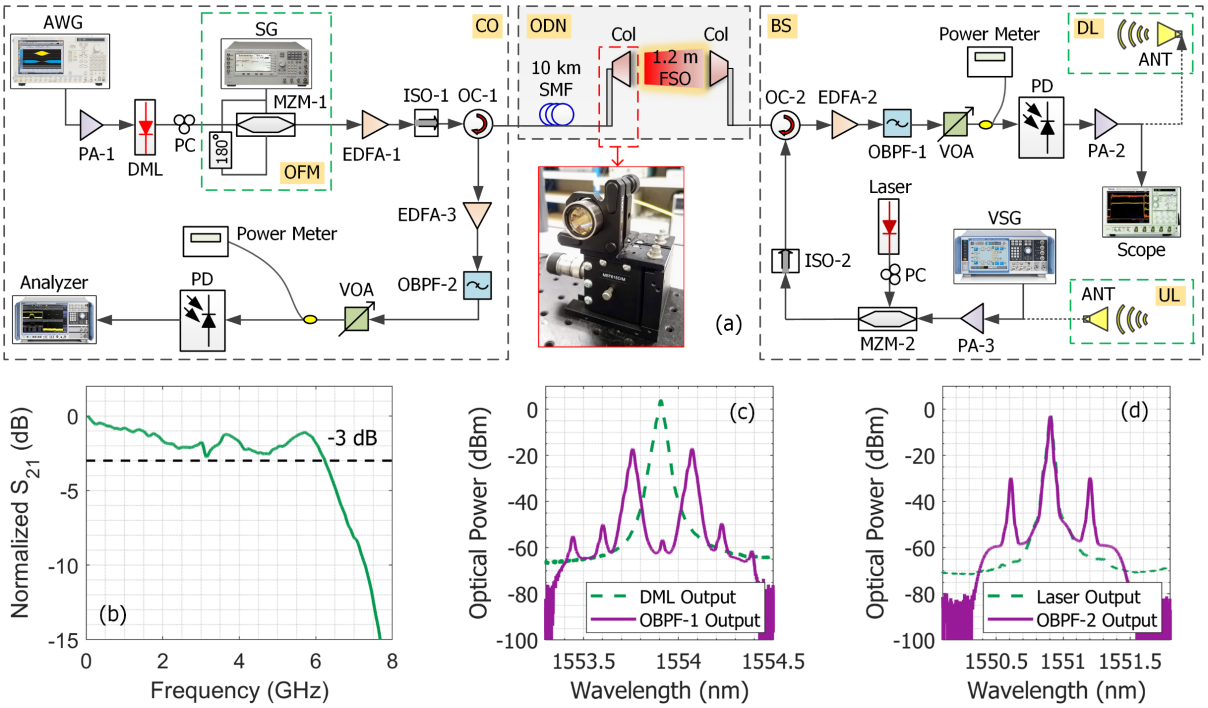

Fig. 4. (a) Experimental setup of the proposed full-duplex HMPL-based 5G mmW FWA networks, (b) DML frequency response, (c) optical spectra measured in DL and (d) optical spectra measured in UL.

saturate them and thus avoid a significant nonlinear distortion. The signal was applied to a non-chirp DML (OpticalZonu OZ516) having a 3 dB-bandwidth of 6 GHz and a fixed power of 5.6 dBm at λ of 1553.9 nm, see Fig. 4(b). The optical spectrum at the DML output is shown in Fig. 4(c). The optical signal was then launched to an OFM module, which can be reused for future high-frequency and high-capacity wavelength-division-multiplexing systems. Here, we adopted the optical frequency doubling based on a dual-electrode MZM (MZM-1, Sumitomo T.DEH1.5-40PD-ADC), biased at the null transmission point (i.e., 9 V) to generate a double-sideband carrier suppressed (DSB-CS) signal. The MZM-1 was driven by a 19.5 GHz input clock signal, generated by a signal generator (SG, Agilent 8267C) via an electrical 180° hybrid coupler. The input clock power was set at 23 dBm. The polarization controller (PC) was used to minimize the polarization-dependent loss. The data-modulated signal was amplified by an erbium-doped fiber amplifier (EDFA-1, Accelink MW series) with a constant gain of 20 dB to compensate for the modulation loss and boost the optical power prior to signal transmission over the optical distribution network (ODN) via the optical isolator (ISO-1) and the directional optical circulator (OC-1) to prevent any signal reflection.

The ODN consisted of a 10 km SMF, the output of which was launched into a 1.2 m FSO link by using a pair of air-spaced doublet collimators (col, Thorlabs F810APC-1550) with an aperture diameter and focal length of 2.54 and 3.71 cm, respectively, see inset in Fig. 4(a). The FSO channel loss was 5.5 dB. The laboratory C_n^2 was about 2.4×10^{-14} $m^{-2/3}$. The ODN output was then transmitted to the BS via an OC-2, amplified by the EDFA-2 (Amonic, AEDFA-23-B-FA) for ODN loss compensation and filtered by an optical bandpass filter (OBPF-1, Finisar WaveShaper 4000S) to reduce amplified spontaneous emission noise. Figure 4(c) also displays the optical spectrum measured after OBPF-1. The frequency spacing between two sidebands is 39 GHz and the measured optical carrier suppression to sideband ratio is 40 dB. A variable optical attenuator (VOA) was then used to reduce the received optical power (P_{r_o}) with respect to the maximum value of 6 dBm into the PIN photodetector (PD, u2t BPDV2020R), where the beating of the two sidebands was held to generate the desired 39 GHz signal. The electrical signal then can be amplified by an mmW PA and radiated wirelessly over the RF link via a grid array of ANTs in real applications. In this work, due to the unavailability of ANTs at 39 GHz band, the signal was then electrically amplified by an IF PA-2 (WNA-180) having 40 dB gain and finally evaluated by a commercially available software (Scope, Tektronix DPO72004C).

For the UL direction, a distributed feedback laser (EXFO IQS-610) emitted the optical power of 12 dBm at λ of 1550.9 nm, whose optical spectrum is shown in Fig. 4(d). It was then connected to a single-drive MZM (MZM-2, Photline MX-LN-40) via a PC for optical modulation. The MZM-2 was biased at the quadrature point (i.e., 5.1 V) to generate a DSB signal. Its modulation operation was driven by a 37 GHz 5G NR signal with 64-QAM at R_b of 2.4 Gb/s, which is the NR- frequency range 2-test model 3.1, generated by a vector signal generator (VSG, R&S SMW200A). The output was amplified by a PA-3 (SHF-810) having 29 dB gain. Note that, the data signal was practically supposed to be transmitted to the MZM-2 after the UL RF transmission. The optical signal was then launched to the mutual ODN via ISO-2 and OC-2. After ODN, it was passed over the OC-1 and VOA then amplified by EDFA-3 (Amonic, AEDFA-23-B-FA) and filtered out by OBPF-2 (AlnairLabs BVF-100), whose spectrum output featuring the DSB is also shown in Fig. 4(d). The optical signal was detected by the PD and finally captured and assessed by a signal and spectrum analyzer (R&S FSW43). The key parameters of the setup are summarized in Tab. 1. To analyze the proposed HMPL, both DL and UL transmission performances are evaluated in terms of EVM, BER, constellation diagrams, P_{r_o} and P_{r_RF} for each QAM signal. Note that the indoor laboratory link was limited by the available space serving as a proof of concept while the link can be scaled up for a real network, as shown further. Also, the system phase noise represents an important issue. However, the systems optically generating mmW signal do not deteriorate significantly phase noise unless long fiber, i.e. over 50 km, or laser with wide linewidth are used [25]. Moreover, the characterization of the phase noise for similar systems can be found in [16].

Table 1. System parameters

Parameter	Value
FSO length	1.2 m
FSO loss	5.5 dB
SMF length	10 km
DL laser	
- wavelength	1553.9 nm
- power	5.6 dBm
UL laser	
- wavelength	1550.92 nm
- power	12 dBm
MZM1 bias voltage	9 V
MZM2 bias voltage	5.1 V
PD responsivity	0.7 A/W
PD 3-dB bandwidth	> 50 GHz
Amplifier noise figure	
- PA-1, PA-2, PA-3	1.6 dB, 2 dB, 6 dB
Amplifier gain	
- PA-1, PA-2, PA-3	25 dB, 40 dB,29 dB

4. EXPERIMENTAL RESULTS AND DISCUSSION

A. DL characterization

To achieve robust multi-user hybrid transmissions at 39 GHz band, the critical point is the determination of optimal IF spectrum in optical back-to-back (OB2B) link (i.e., no ODN). Figure 5(a) therefore presents the EVM performance of a single-band signal i.e., single user (4 Gb/s 16-QAM) at different IF ranging from 1 GHz to 5 GHz with a step of 0.5 GHz. Also shown is the EVM required limit of 12.5% for 16-QAM [26]. As expected, the EVM performance, in general, is degraded when the IF increases. The measured EVM value of about 5.0% is achieved for IF ranging from 1 to 3 GHz. However, for IF set from 3.5 to 5 GHz, we notice a significant increase of EVM performance from 8.3 to 36.0%. At IF of 4 GHz, the signal fails to satisfy the EVM requirement. This EVM performance limitation is mostly due to (*i*) the response of the AWG, which has an operational bandwidth of 4.8 GHz and (*ii*) PA-1, whose operation bandwidth is in the low frequency range from 20 MHz to 3 GHz. To verify the effect, we measured the EVM performance in the electrical B2B (EB2B) configuration, which has EVM performances well below the required limit for all IFs.

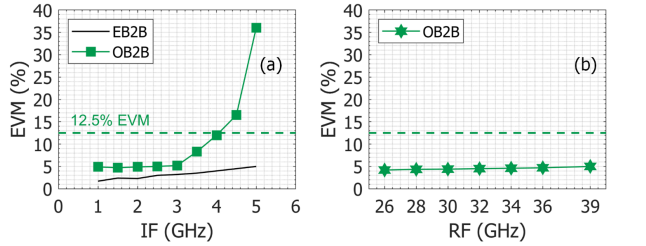

Fig. 5. Measured EVM at different (a) IF and (b) RF in OB2B configuration.

To examine the signal quality at different 5G-envisioned RFs below 39 GHz, we then show in Fig. 5(b) the respective EVM performances for RFs ranging from 26 to 36 GHz with 2 GHz step. Note that, the IF was set at 2.5 GHz for all cases. As expected, when increasing the RF from 26 to 36 GHz, the corresponding EVM value is slightly degraded with only 0.5% EVM penalty, which verifies the benefit of the OFM technique for flexibly generating the optical mmW signal.

B. DL performance

As a proof-of-concept demonstration, the transmission of three-band SCM signals (each band represents one user – 1 Gb/s per user) based on the variable QAM allocations scheme over OB2B, 10 km SMF and hybrid links is experimentally evaluated. The SCM signal consists of 64-, 16- and 4-QAM centered to the IF of 2 GHz, 2.5 GHz and 3 GHz, respectively (0.5 GHz guard band). Prior to carrying out measurements for the three-band transmission, we first measured the link performance for the single-band signal (i.e., single user – 4 Gb/s 16-QAM at the IF of 2.5 GHz).

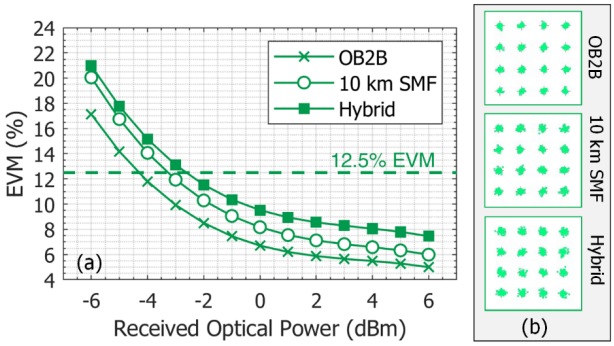

Fig. 6. (a) Measured EVM versus received optical power for a single user – 4 Gb/s 16-QAM. (b) constellation diagrams for OB2B, SMF and hybrid configurations.

Figure 6(a) depicts the link performance in terms of EVMs for a wide range of P_{r_o} of the single-band signal. As shown, the EVM plots display the exponential drop with P_{r_o} for all transmission scenarios. The EVM value for OB2B measured at P_{r_o} of 6 dBm are 5.0%, while that of 10 km SMF and hybrid links are 6.0 % and 7.5%, respectively, resulting in the EVM penalties of 1 and 2.5%, compared to OB2B. Comparing at the required EVM limit, for OB2B and 10 km SMF link, they are met at the respective P_{r_o} of -4.3 dBm and -3.3 dBm, i.e., only 1 dB optical power penalty. Including the FSO channel caused the optical power degradation by only 0.8 dB, which verifies the effective use of FSO channel in the bidirectional HMPL with the mutual ODN for DL and UL. We further confirm the high-quality transmission of the single-band signal by measuring the constellation diagrams at P_{r_o} of 6 dBm, which are very clear for all three scenarios, see Fig. 6(b).

For three-band scenario (1 Gb/s each), the measured EVMs versus P_{r_o} of the SCM signals after OB2B and hybrid transmissions are shown in Fig. 7(a) and (b), respectively. As can be seen, all signals satisfy the EVM requirements for both configurations. For OB2B, the lowest EVMs for 4-, 16- and 64-QAM are 7.5%, 4.5% and 3.6%, respectively. The EVM performances are considerably less than the respective EVM requirements. The corresponding received RF spectrum and constellation diagrams are displayed in Fig. 7(c), which are clear and discernible.

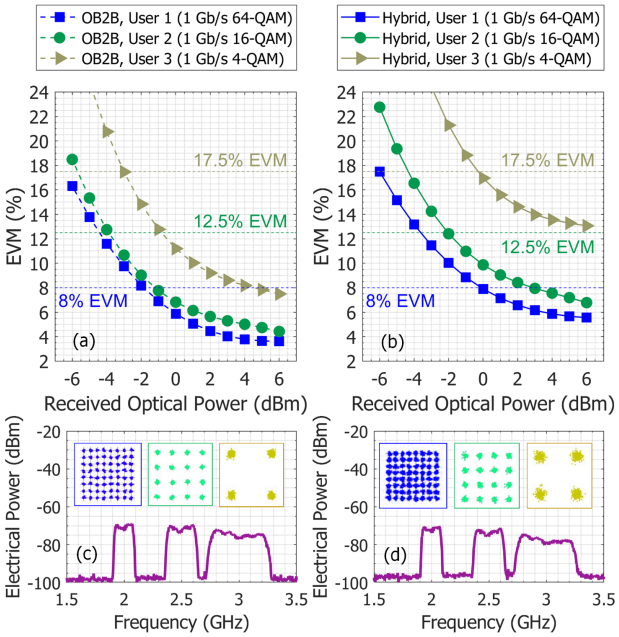

Fig. 7. Measured EVM versus received optical power for each band after (a) OB2B and (b) hybrid transmissions. (c) – (d) are the corresponding received RF spectra and constellation diagrams (as insets) of OB2B and hybrid transmissions, respectively.

Under the hybrid condition, at P_{r_o} of 6 dBm, the measured EVMs are 13.1%, 6.7% and 5.5% for 4-, 16- and 64-QAM, respectively i.e., satisfying well the 3GPP specifications. The resultant EVM penalties between OB2B and hybrid transmissions are 5.6%, 2.2% and 1.9% for 4-, 16- and 64-QAM, respectively. This can be attributed to the CD (set to 17 ps/(nm·km)) and FSO loss, which degrade the signal-to-noise ratio (SNR) as shown in the received RF spectrum in Fig. 7(d), where we noticed the spectrum profile is tilted, the noise floor is increased and the received power is reduced gradually for bands at higher IFs. Still, the performance of the SCM signals is generally satisfactory, validating the effectiveness of using the variable QAM allocations scheme for delivering different multi-Gb/s signals over the hybrid link. Bearing in mind the availability of signal spectrum and selection of IF with narrower guard band – subject to the optimum QAM employed, more users can be accommodated based on the variable QAM allocations technique. In addition, we further observe two key points:

i. By transmitting the SCM signals, the intermodulation effect is noticeable. For example, for OB2B, comparing the 1 Gb/s 16-QAM in SCM signals (4.5% EVM at P_{r_o} of 6 dBm) to that of single-band signal, whose EVM value is 5.0% but at R_b of 4 Gb/s, see Fig. 6(a). Nevertheless, the satisfactory performance of SCM signals over the hybrid link is also achieved.

ii. Although the EVM performances of 4-QAM in SCM signals for both OB2B and hybrid links are below 17.5% EVM criterion, it is still high in comparison to that of 16- and 64-QAM. This is mainly because part of 4-QAM signal spectrum is out of the maximum frequency range of PA-1, which transfer response is non-flat and therefore significantly deteriorated signal beyond 3 GHz (see Fig. 7(c) and (d)). Due to this issue, the outer symbols of 4-QAM constellations are randomly spread, which can be observed in the insets of Fig. 7(c) and (d), respectively, while 16- and 64-QAM constellations are visibly concentrated.

To further evaluate the DL performance, we present the BER performance as a function of received RF power (P_{r_RF}). This measurement is critical in order to determine S_{Rx}, whose parameter is used to estimate L_{RF}. The BER curves, which are calculated based on the measured EVM values for the SCM signals in the hybrid condition, are illustrated in Fig. 8. As can be seen, all bands show the best BER below the forward error correction (FEC) threshold of 3.8×10^{-3}. The S_{Rx} for 4-QAM is about -32 dBm, while that of 16- and 64-QAM are about -28 dBm and -24 dBm suffering the RF power penalties of 4 dB and 8 dB, respectively, in comparison to 4-QAM owing to its higher-order nature.

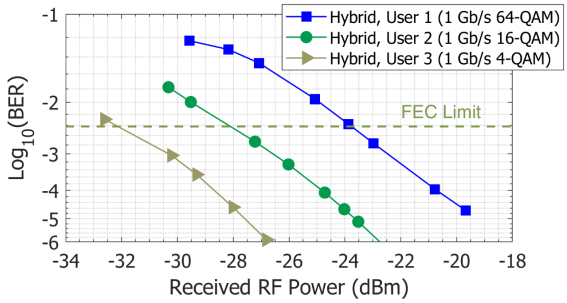

Fig. 8. Calculated BER versus received RF power for each band after hybrid transmission.

C. UL performance

In UL, for the first time, we transmit directly the 37 GHz 5G NR signal with 64-QAM at R_b of 2.4 Gb/s over the bidirectional and mutual ODN with DL. Note that, when measuring the UL performance, DL was also turned on, which is crucial in a practical sense. It is worth mentioning that for the UL transmission, the measured input RF power with respect to the required EVM limit (dynamic range measurement) is critical. This is because, in practical implementations, the signal performance is certainly degraded by the RF wireless link – not even taking into account the rain effect. Therefore, the more rigorous requirement is set at the Tx, the superior performance is ensured at the Rx.

Since the RF wireless link was not constructed in our proposed HMPL due to the unavailability of ANTs, the input RF power is therefore emulated by the power produced by VSG, showed in Fig. 4(a). The results measured in the OB2B condition are depicted in Fig. 9, where we achieve the dynamic range of 14 dB and the lowest EVM value of 3.5% at an input RF power of -18 dBm, which was also adopted for all transmission scenarios.

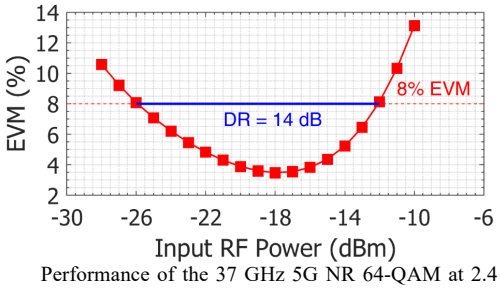

Fig. 9. Performance of the 37 GHz 5G NR 64-QAM at 2.4 Gb/s as a function of input RF power. DR: dynamic range.

We then examined the system stability of the UL when DL was turned on. Note that, for this measurement, only the FSO channel was in the ODN. Figure 10 shows the stability results, where we observe almost the same EVM of 3.68% (i.e., considerably less

than the 8% EVM criterion) over 25-minute period. No optical reflection and interference effects were observed due to the DL, which confirms the proposed full-duplex system is stable and practical for operation.

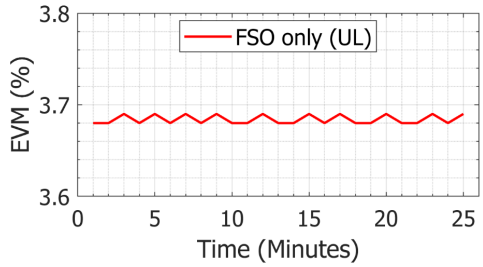

Fig. 10. FSO stability in UL direction with 2.4 Gb/s 64-QAM.

Figure 11(a) shows the EVM performance as a function of P_{r_o} for OB2B, 10 km SMF, and hybrid links. As illustrated, we achieve robust transmissions for the UL signal, e.g., at P_{r_o} of 6 dBm, the measured EVMs for OB2B, 10 km SMF and hybrid link are 3.5%, 3.8% and 4.1%, which are well below the 8% EVM criterion.

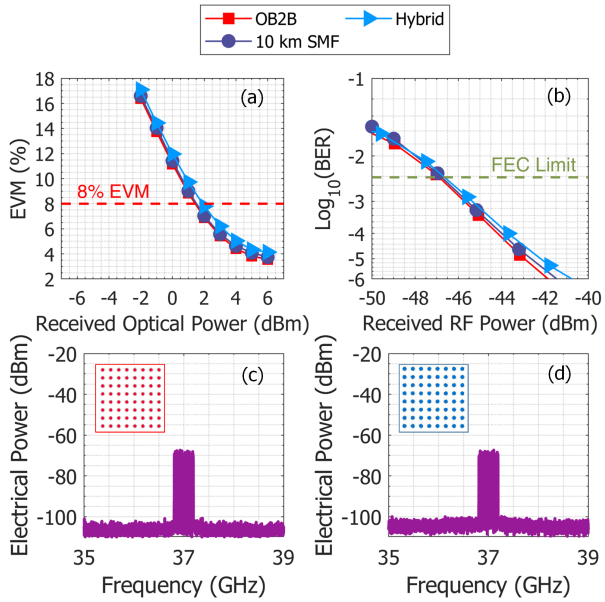

Fig. 11. (a) Measured EVM versus the received optical power and (b) calculated BER versus received RF power after OB2B, 10 km SMF and hybrid transmissions. (c) – (d) are the received RF spectra and constellation diagrams for OB2B and hybrid links, respectively.

The EVM penalties are insignificant since they are less than 0.6%. Compared to the required EVM limit of 8%, the measured P_{r_o} for OB2B is 1.5 dBm while that for 10 km SMF and hybrid links are about 1.5 dBm and 2 dBm, indicating almost no optical power penalties.

To further evaluate the performance of the UL transmission, we present in Fig. 11(b) the BER performance versus P_{r_RF}, which was directly measured at 37 GHz. All cases show the best BERs below the FEC threshold with almost no RF power penalties compared to the FEC limit. The S_{Rx} for 64-QAM is determined about -47 dBm. The received RF spectra and constellation diagrams at P_{r_o} of 6 dBm are shown in Fig. 11(c) and (d) for OB2B and hybrid configurations, respectively. They are stable and clear. These results confirm the feasibility of using the DSB scheme for UL transmission in the proposed full-duplex HMPL. It is anticipated that, the UL signal can be successfully transmitted over the hybrid channel with longer L_{FSO} by using the commercial FSO transceivers owing to their high-quality transmission performance.

D. Estimation of maximum DL and UL RF transmission length

In our experimental setup, we used only the optical part of the HMPL, i.e., without antenna channel. However, to evaluate the performance of the proposed HMPL with the seamless three-stage system (SMF, FSO and RF wireless link) in a complete manner, in this section we present calculated results of the achievable L_{RF} of the SCM and 5G NR signals in DL and UL, respectively. The L_{RF} estimation is based on the commercial ANTs, practical transmit powers (P_t) at the ANT and minimum P_{r_RF} required to meet the FEC limit (i.e., receiver sensitivity S_{Rx}) as observed from measurements in Fig. 8 and 11(b). It can be calculated based on the Friis transmission equation. The S_{Rx} is given by [27]:

$$S_{Rx} = P_t + G_{Tx} + G_{Rx} - 20\log_{10}(\alpha_{PT}) - (\alpha_{atm\_RF} + \alpha_{rain})L_{RF} - M \quad (3)$$

where G_{Tx}, G_{Rx} and M are the Tx, Rx ANT gains and link margin, respectively, α_{atm_RF} is the atmospheric attenuation factor of RF link and α_{PT} is propagation path loss.

As can be seen, L_{RF} is highly dependent on the designed link margin and the amount of attenuation due to rainfall. The former is reserved and set at 5 dB for compensation of other effects, while the latter is related to the availability concept that can be determined using statistical rainfall data over a long period of time in a specific area. To maintain a high reliablity in the RF wireless link, an availability of 99.999% (five-nine) is required. In this work, we adopt in simulations α_{rain} of 34 dB/km (99.999%), which is considered as heavy rain based on the data set of rain rate measurement for three-year duration in Vigo, Spain at 39 GHz [28].

We then could estimate the maximum L_{RF} for both DL and UL based on the specifications given in Table 2. Note that, P_{t_RF} and G_T for UL are practically set lower than that of DL. This is because, at 39 GHz band, the maximum effective isotropic radiated power i.e., $P_t + G_{Tx}$ is regulated to be 43 dBm by the US Federal Communications Commission [29].

Table 2. Link budget for both DL and UL RF wireless transmission to guarantee 99.999% availability.

Parameters	DL SCM signal (4/16/64-QAM)	UL 5G NR signal (64-QAM)
Transmit power (dBm)	20, 30	5, 10
Tx ANT gain (dBi)	40	30
Rx ANT gain (dBi)	30	40
Atmospheric loss (dB/km)	0.18	0.18
Link margin (dB)	5	5
Rain loss (dB/km)	34	34
Receiver sensitivity (dBm)	-32/-28/-24	-47

Figures 12(a) and (b) then show the estimated L_{RF} for DL in the fair weather (no rain) and rain conditions. Fig. 12 also shows the measured S_{Rx} levels of 4-, 16- and 64-QAM. As can be seen, for higher-order QAM signals, L_{RF} is shorter owing to the stringent requirement on the P_{r_RF} and SNR. With P_t of 20 dBm,

the SCM signals generally satisfy a minimum L_{RF} of 150 m for the case of no rain while that under the rain is 100 m. Increasing P_t to 30 dBm, the corresponding minimum L_{RF} values are extended up to 500 m and 200 m. Using the same approach as that of the DL, L_{RF} for the 5G NR signal in UL is also predicted, see Fig. 13. The results show that at P_t of 10 dBm, without rain, L_{RF} is longer than 700 m while that under the rain is 250 m. These simulation-based results indicate that under the heavy rain condition in Spain, for guaranteeing 99.999% availability, the minimum L_{RF} for both DL and UL is 200 m, which is sufficient for 5G small-cell coverage.

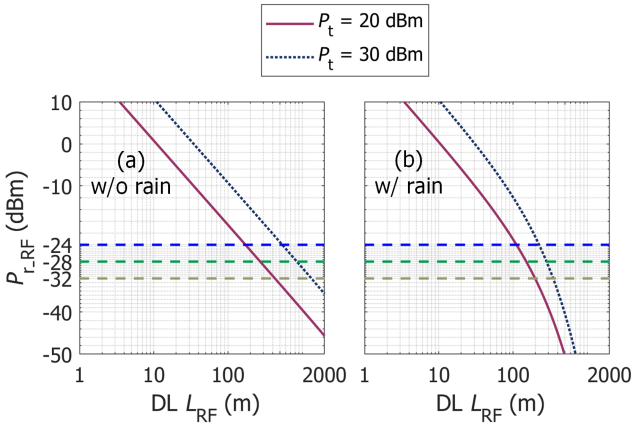

Fig. 12. Simulation results of achievable wireless DL length with different P_t values for (a) no rain and (b) rain in Spain to get availability level of 99.999% based on three-year measurement period.

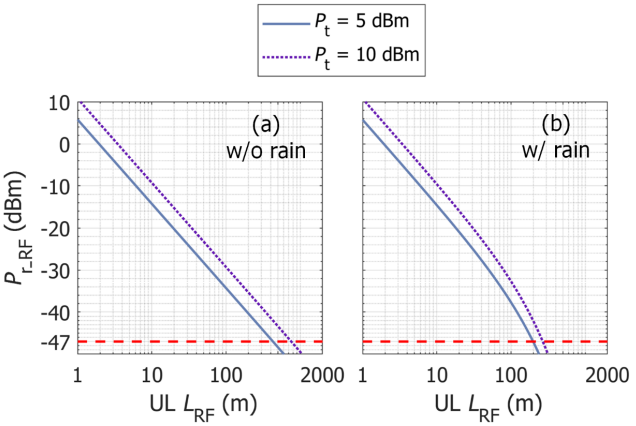

Fig. 13. Simulation results of achievable wireless UL length with different P_t values for (a) no rain and (b) rain in Spain to get availability level of 99.999% based on three-year measurement period.

5. SIMULATION ANALYSIS FOR EXTENDED LINK

Because of the equipment limitations in the DL, we could transmit three-band SCM signals with only 1 Gb/s per each one over the proposed system to prove the concept. To allow for more detailed understanding of the uniform and variable QAM allocations featuring multi-user service with higher R_b and longer L_{FSO}, we thus construct a system model based on OptiSystem-MATLAB co-simulation platform to closely resemble the experimental setup shown in Fig. 4(a). Note that, for practical implementations, the FSO channel was thus represented by commercial FSO transceivers' parameters with d_T and d_R of 10 cm and θ of 0.55 mrad [12]. We also set in FSO channel the C_n^2 of 10^{-15} $m^{-2/3}$, which is a moderate value in outdoor environments. It is worth mentioning that, the effect of both AWG and PA-1 bandwidth limitation was not considered in the simulation. For simplicity, all simulated EVM results are achieved at P_{r_o} of 6 dBm for a fair comparison between uniform and variable QAM allocations schemes.

A. Multi-user link with uniform QAM allocations

Given the specific IF within 1 to 5 GHz as presented in Fig. 5(a), it is therefore straightforward to deliver an aggregate R_b of 10 Gb/s accommodating at least five users – 2 Gb/s per user by employing five-band SCM signals. This is to improve the R_b of 1.5 Gb/s, which is currently established in smart industries [1]. The respective IFs for each band are 1 GHz, 2 GHz, 3 GHz, 4 GHz and 5 GHz – having the guard band of 1 GHz. We used this multi-band SCM as an example of the possible multi-band signal arrangement to evaluate the performance of the hybrid system.

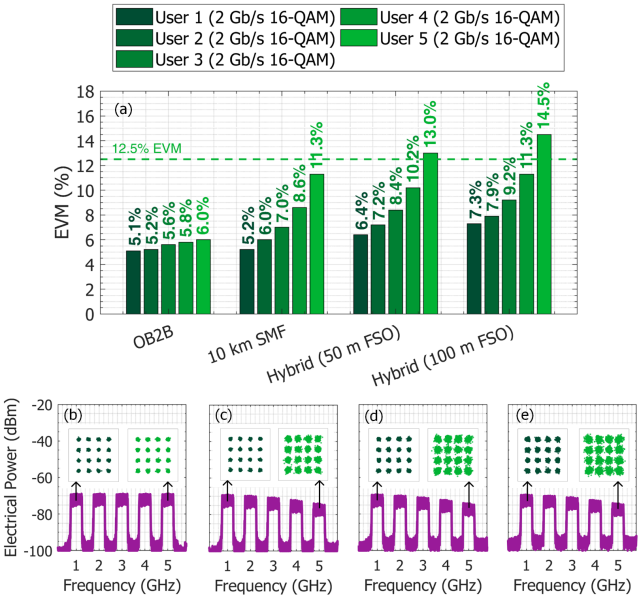

Fig. 14. (a) Simulated EVM performance for 10 Gb/s five-band 16-QAM after OB2B and hybrid transmissions. (b) – (e) are the received RF spectra for OB2B, 10 km SMF, hybrid (10 km SMF, 50 m FSO) and hybrid (10 km SMF, 100 m FSO), respectively. Insets are the received 16-QAM constellation diagrams for band #1 and #5.

As the first set of simulations, all five bands of the SCM stream were modulated with 16-QAM. As can be seen in Fig. 14(a), for OB2B, the simulated EVMs for band #1 and #5 are 5.1% and 6.0%, respectively, which leads to 0.9% EVM penalty. The received RF spectrum is displayed in Fig. 14(b), where we observe a steady and similar profile for all five bands without noticeable distortions. Also shown in Fig. 14(b) are the insets, which illustrate clear constellation diagrams of bands #1 and #5. For the 10 km SMF transmission, an EVM penalty of 6.1% is observed between bands #1 and #5. This is especially due to the CD-induced power fading, which is more severe for higher IFs since the signal power periodically fades with the increase of the carrier frequency. The effect can be clearly observed via the received RF spectrum depicted in Fig. 14(c), whose trend is similar to the experiments e.g., tilted spectrum profile, reduced received power and increased noise floor. The corresponding constellations are thus distorted, but still separated clearly. However, for hybrid transmission with L_{FSO} of 50 m and 100 m, only the first four users can be accommodated since band #5 has the corresponding EVM values of 13.0% and 14.5%, which fails to meet the 12.5% EVM requirement. The

corresponding constellations are therefore further spread due to the SNR degradation i.e., increased noise floor.

In the second set of simulations, we upgraded all five bands of the SCM signal to 64-QAM. The R_b of each remained at 2 Gb/s with the bandwidth occupancy of 0.33 GHz. As shown in Fig. 15(a), we observe an EVM between 5.6 – 6.4% (below the required EVM limit of 8%) for all bands in the OB2B scenario. Corresponding constellation diagrams are discernible; see inset in Fig. 15(b). However, we notice that for 10 km SMF and hybrid links with L_{FSO} of 50 m and 100 m, only three and two users can be facilitated, respectively.

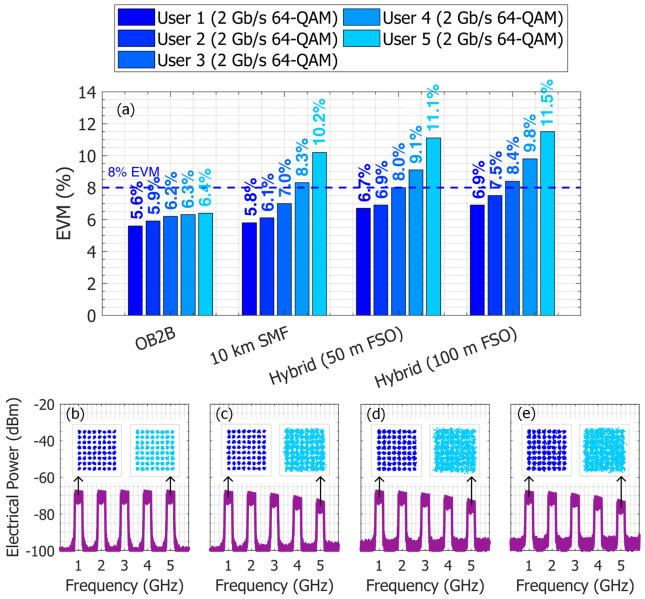

Fig. 15. (a) Simulated EVM performance for 10 Gb/s five-band 64-QAM after OB2B and hybrid transmissions. (b) – (e) are the received RF spectra for OB2B, 10 km SMF, hybrid (10 km SMF, 50 m FSO) and hybrid (10 km SMF, 100 m FSO), respectively. Insets are the received 64-QAM constellation diagrams for band #1 and #5.

B. Multi-user link with variable QAM allocations

The implementation of the HMPL using the uniform QAM allocations is not practical since the delivery of 10 Gb/s five-band SCM signals over the hybrid link with L_{FSO} of at least 50 m is not reachable. To overcome this problem, it is highly desirable to employ the variable QAM allocation scheme, where different QAMs are applied on the composite SCM signal to facilitate multi-user service.

Therefore, in the next simulation set, following similar IF settings, we then assigned 4-QAM for band #5, 16-QAM for band #2, #3 and #4 and 64-QAM for band #1 in order to effectively deliver a sum R_b of 10 Gb/s to five users. The results are shown in Fig. 16(a). As can be seen, a performance improvement is evidently achieved when using the variable QAM allocations. Corresponding constellations are well separated for all QAMs, see Fig. 16(c). For the hybrid link with L_{FSO} extended to 200 m, four users can also be accommodated since the EVM performance of band #5 is 17.7%, which is slightly above the 17.5% criterion.

It is also worth mentioning that a good agreement is achieved between the experimental testbed and constructed simulation performances, e.g., for OB2B, the simulated EVM value of 16-QAM at the IF of 3 GHz is 4.7%. This is slightly higher than that of measurements e.g., 4.5% since R_b in simulation is 2 Gb/s – see Fig. 7(a). These imply the feasibility of the SCM signals to be transmitted over longer L_{FSO} (i.e., 150 m) by using the commercial FSO transceivers for practical applications. One may note that within the specific IF between 1 and 5 GHz, by using the variable QAM allocation technique, a larger number of users (2 Gb/s per user) can be achieved depending on the guard band between SCM signals. Figure 17 shows the received RF spectrum in the OB2B condition with seven users (14 Gb/s in total), where we map 4-QAM at IF of 1 GHz, 16-QAM at IF of 1.55 GHz, 2.15 GHz, 2.75 GHz, 3.35 GHz and 3.95 GHz and 64-QAM at IF of 4.8 GHz. Due to the dense allocation, the EVM performances in OB2B scenario for all bands are slightly high triggered by the intermodulation effect but still well below the corresponding required EVM limits, which can be observed by the clear constellation diagrams.

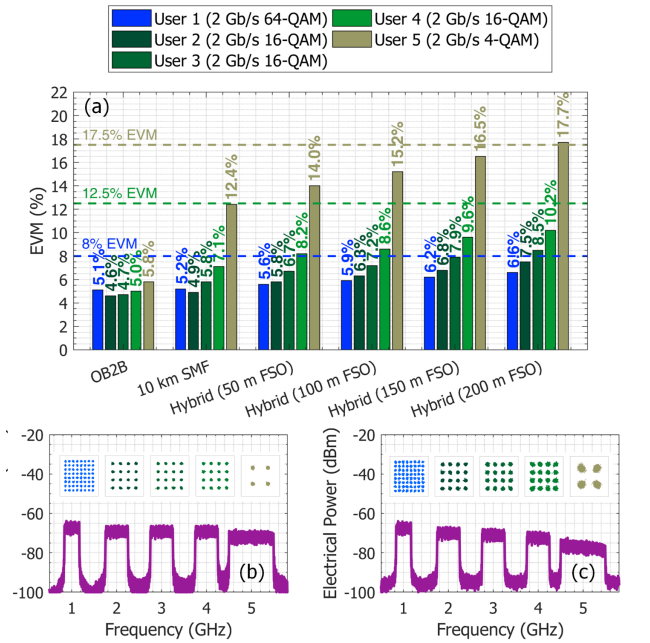

Fig. 16. (a) Simulated EVM performance for 10 Gb/s five-band with variable QAM allocation after OB2B and hybrid transmissions. (b) – (c) are the received RF spectra observed after OB2B and hybrid (10 km SMF, 150 m FSO) transmissions, respectively. Insets show the received QAM constellation diagrams for each band.

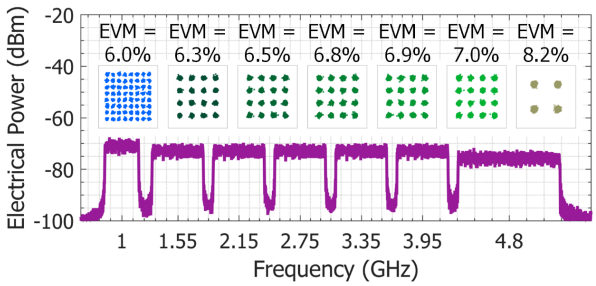

Fig. 17. Received RF spectrum of 14 Gb/s 7-band variable-QAM after OB2B transmission. Also shown in insets are the constellation diagrams of each band with correspoding EVM performance.

It is also worth mentioning that this mapping was used as a reference; more users can also be accommodated considering the availability of signal spectrum from 0 to 1 GHz – subject to the optimum QAMs employed. However, the transmission of multi-user over fiber and hybrid links using the variable QAM

allocations in a dense setting is not in the scope of the work presented here.

6. CONCLUSIONS

We have proposed a hybrid full-duplex microwave photonic links for mmW 5G RAN to support the Industry 4.0 connectivity requirements in a cost-effective (e.g., DML deployment and mutual ODN between DL and UL) and flexible (e.g., OFM module) manner. Through the experimental results obtained, the further extension by numerical simulation analysis provided verification of fruitfully realized transmissions of 10 Gb/s SCM signals in the DL and 2.4 Gb/s 5G NR signal in the UL over 10 km SMF, 150 m FSO and 200 m RF wireless link under heavy rain conditions based on the available data from Spain. The achieved EVMs and BERs for all DL and UL signals are well below the required limits defined by the 3GPP standards and FEC threshold, respectively. The presented results confirm the potential use of the proposed three-stage system to provide high-speed broadband services in the suburban areas, where most manufacturing plants and factories are typically located.

Future work will include investigations of the multiband transmission over the SMF/FSO/RF link using the variable QAM allocations in a dense setting to accommodate more users.

Acknowledgement

This work is supported by COST Action CA19111 NEWFOCUS and CTU project SGS20/166/OHK3/3T/13.

Disclosures

The authors declare no conflicts of interest.

Data Availability

Data underlying the results presented in this paper are not publicly available at this time but may be obtained from the authors upon reasonable request.

References

[1] Qualcomm, “Deploying 5G NR mmWave to unleash the full 5G potential,” Qualcomm (2020), https://www.qualcomm.com/media/documents/files/deploying-mmwave-to-unleash-5g-s-full-potential.pdf

[2] “5G spectrum GSMA public policy position,” 2020. [Online]. Available: https://www.gsma.com/

[3] D. Thalakotuna and K. P. Esselle, “Overcoming 5G millimeter wave black holes,” *IEEE Futur. Networks Tech Focus*, vol. 3, no. 3, 2019.

[4] M. Sung *et al.*, “RoF-based radio access network for 5G mobile communication systems in 28 GHz millimeter-wave,” *J. Lightwave Technol.*, vol. 38, no. 2, pp. 409–420, 2020.

[5] A. Bekkali, T. Kobayashi, K. Nishimura, N. Shibagaki, K. Kashima, and Y. Sato, “Millimeter-wave-based fiber-wireless bridge system for 8K UHD video streaming and gigabit ethernet data connectivity,” *J. Lightwave Technol.*, vol. 36, no. 18, pp. 3988–3998, 2018.

[6] R. K. Shiu *et al.*, “Optical signal processing for W-band radio-over-fiber system with tunable frequency response,” *IEEE J. Sel. Top. Quantum Electron.*, vol. 27, no. 2, 2021.

[7] S. Rommel, D. Perez-Galacho, J. M. Fabrega, R. Munoz, S. Sales, and I. Tafur Monroy, “High-capacity 5G fronthaul networks based on optical space division multiplexing,” *IEEE Trans. Broadcast.*, vol. 65, no. 2, pp. 434–443, 2019.

[8] H. Y. Wang, C. H. Cheng, C. T. Tsai, Y. C. Chi, and G. R. Lin, “Multi-color laser diode heterodyned 28-GHz millimeter-wave carrier encoded with DMT for 5G wireless mobile networks,” *IEEE Access*, vol. 7, pp. 122697–122706, 2019.

[9] Q. Zhou *et al.*, “Centralized digital self-interference cancellation technique to enable full-duplex operation of next generation millimeter wave over fiber systems,” in *Optical Fiber Communication Conference*, 2020, p. Th2A.46.

[10] J. Kim *et al.*, “MIMO-supporting radio-over-fiber system and its application in mmWave-based indoor 5G mobile network,” *J. Lightwave Technol.*, vol. 38, no. 1, pp. 101–111, 2020.

[11] C. Lim, Y. Tian, C. Ranaweera, A. Nirmalathas, E. Wong, and K. Lee, “Evolution of radio-over-fiber technology,” *J. Lightwave Technol.*, vol. 37, no. 6, pp. 1647–1656, 2019.

[12]] A. K. Majumdar, Z. Ghassemlooy, A.A. B. Raj, Principles and Applications of Free Space Optical Communications, The Institution of Engineering and Technology, 2019.

[13] Y. Alfadhli *et al.*, “Real-time FPGA demonstration of hybrid bi-directional MMW and FSO fronthaul architecture,” in *Optical Fiber Communication Conference*, 2019, p. W2A.39.

[14] P. T. Dat *et al.*, “High-speed radio-on-free-space optical mobile fronthaul system for ultra-dense radio access network,” in *Optical Fiber Communication Conference*, 2020, p. W2A.37.

[15] C. H. de S. Lopes *et al.*, “Non-standalone 5G NR fiber-wireless system using FSO and fiber-optics fronthauls,” *J. Lightwave Technol.*, vol. 39, no. 2, pp. 406–417, Jan. 2021.

[16] J. Bohata, et al., "Experimental comparison of DSB and CS-DSB mmW formats over a hybrid fiber and FSO fronthaul network for 5G," Opt. Express, vol. 29, pp. 27768-27782, Aug. 2021.

[17] [11]D.-N. Nguyen, et al., "M-QAM transmission over hybrid microwave photonic links at the K-band," Opt. Express, vol. 27, no. 23, pp. 33745-33756, Nov. 2019.

[18] L. Vallejo, B. Ortega, D.-N. Nguyen, J. Bohata, V. Almenar, and S. Zvanovec, “Usability of a 5G fronthaul based on a DML and external modulation for M-QAM transmission over photonically generated 40 GHz,” *IEEE Access*, vol. 8, pp. 223730–223742, 2020.

[19] L. C. Andrews and R. L. Phillips, *Laser beam propagation through random media*, vol. 1. 1000 20th Street, Bellingham, WA 98227-0010 USA: SPIE, 2005.

[20] ITU-R P.676-11, “Attenuation by atmospheric gases,” 2016.

[21] M. Huang, Y. Chen, R. Shiu, H. Wang, and G.-K. Chang, “A bi-directional multi-band, multi-beam mm-wave beamformer for 5G fiber wireless access networks,” *J. Lightwave Technol.*, vol. 39, no. 4, pp. 1116–1124, Feb. 2021.

[22] E. Ruggeri *et al.*, “A 5G fiber wireless 4Gb/s WDM fronthaul for flexible 360° coverage in V-band massive MIMO small cells,” *J. Lightwave Technol.*, vol. 39, no. 4, pp. 1081–1088, Feb. 2021.

[23] N. Anand, K. Sunilkumar, S. K. Satheesh, and K. Krishna Moorthy, "Entanglement of near-surface optical turbulence to atmospheric boundary layer dynamics and particulate concentration: implications for optical wireless communication systems," *Appl. Opt.*, vol. 59, pp. 1471-1483, 2020.

[24] M. A. Esmail, H. Fathallah, M. S. Alouini, "Outdoor FSO

communications under fog: attenuation modeling and performance evaluation, " *IEEE Photonics Journal*, vol. 8, no. 4, pp. 1-22, 2016.

[25] G. Qi, J. Yao, J. Seregelyi, S. Paquet, C. Belisle, X. Zhang, K. Wu and R. Kashyap, "Phase-noise analysis of optically generated millimeter-wave signals with external optical modulation techniques," Journal of Lightwave Technology, vol. 24, no. 12, pp. 4861-4875, 2006.

[26] 3GPP TS 138 101-1, "5G NR User Equipment (UE) radio transmission and reception," 2018.

[27] P. T. Dat, A. Kanno, K. Inagaki, and T. Kawanishi, "High-capacity wireless backhaul network using seamless convergence of radio-over-fiber and 90-GHz millimeter-wave," *J. Lightwave Technol.*, vol. 32, no. 20, pp. 3910–3923, 2014.

[28] D. (Das) Nandi, F. Pérez-Fontán, V. Pastoriza-Santos, and F. Machado, "Application of synthetic storm technique for rain attenuation prediction at Ka and Q band for a temperate Location, Vigo, Spain," *Adv. Sp. Res.*, vol. 66, no. 4, pp. 800–809, 2020.

[29] "Report and order and further notice of proposed rulemaking," 2016. [Online]. Available: https://docs.fcc.gov/public/attachments/FCC-16-89A1.pdf.